Simulation of granular friction and its effective theory

Hisao HAYAKAWA *)

Graduate School of Human and Environmental Studies, Kyoto University, Kyoto 606-8501

(Received)

This paper discusses the application of the distinct element method (DEM) for granular friction and its effective (or simplified) macroscopic models. We focus on the stick-slip motion in a sheared granular friction process which correspond to an experiment by Nasuno et al. (Phys. Rev. E **58** (1998) 2161). We reproduce many of their experimental results from the simulations of the DEM model and the effective model.

§1. Introduction

Unlike usual solids, liquids or gases, granular materials are known to show complex dynamical behaviors[1]. Frictions in granular layers include essential characteristics of the granular rheology such as the coexistence of a fluid-like phase and a solid-like phase, and their conversion with each other[2]. The simplest situation under the consideration by Nasuno et al.[3] is as follows: Let a plate place on granular layers, and push the plate with a constant speed. When the speed is low, we can observe stick-slip motion of the plate, while the speed is high we can see a steady sliding of the plate. Similar behaviors have been observed even in atomic dry friction[4] and melt fracture of polymers[5]. From a sensitive measurements of frictional forces in granular particles, Nasuno et al.[3] found that the frictional force is a multi-valued and exhibits a hysteresis. They also reported a universal form in instantaneous velocity profile during slip in stick-slip regime.

In this paper, we reproduce some of phenomena observed by Nasuno et al.[3] from both a microscopic simulation based on distinct element method (DEM) and a macroscopic phenomenological model[6]. We expect that our numerical work is helpful to understand the mechanism of granular friction.

The organization of this paper is as follows. In the next section, we will apply DEM to granular frictions. In section 3, we will introduce our phenomenological model , and will present the result of our simulations. In section 4, we will give concluding remarks.

§2. DEM simulation

The distinct element method (DEM) is a soft-core molecular dynamics including dissipation during collisions among particles. Since the proporsal by Cundall and Strack[7], this method is accepted as a standard one to simulate granular motion quantitatively. Granular frictions under the shear force have been simulated

*) E-mail address: hisao@yuragi.jinkan.kyoto-u.ac.jp

typeset using $\mathcal{PTP}$TEX.sty <ver.1.0>

by Thompson and Grest[8], and Matthey and Hansen[9]. In particular, the former situation corresponds to that by Nasuno et al[3]. However, the author tries to reproduce the process with the aid of DEM, because (i) DEM is helpful to understand the mechanism and to construct a phenomenological model, and (ii) the previous simulations[8),9)] do not include the rotation of particles.

The basis of DEM is Herzian contact theory[10]. There is the relation between the compressed force F_n and the normal deformation δ_n, when two identical particles with their diameter d are contacted with each other:

$$F_n = \frac{E}{3(1-\sigma_0^2)}\delta_n^{3/2} = k_n(\delta_n)\delta_n, \tag{2·1}$$

where σ_0 and E are respectively the Poission ratio and the Young modulus. The tangential elastic contact force is given by[11]

$$F_t = \frac{E\sqrt{d\delta_n}}{(2-\sigma_0)(1+\sigma_0)}\delta_t = k_t(\delta_n)\delta_t, \tag{2·2}$$

where suffix t represents the tangential counter parts of suffix n (normal ones).

Now let us consider a collection of monodisperse spherical particles. Here, we assume that each particle has the diameter d, the mass m and the momentum of inertia $I = md^2/10$. The equations of motion for this system are given by

$$\begin{aligned} m\ddot{\mathbf{x}}_i &= \sum_{<i,j>} \theta(d - |\mathbf{x}_i - \mathbf{x}_j|)(\tilde{\mathbf{F}}_n^{ij} + \tilde{\mathbf{F}}_t^{ij}) \\ I\dot{\omega}_i &= \frac{d}{2}\sum_{i,j} \theta(d - |\mathbf{x}_i - \mathbf{x}_j|)(\mathbf{n} \times \tilde{\mathbf{F}}_t^{ij}), \end{aligned} \tag{2·3}$$

where $\theta(x) = 1$ for $x > 0$ and $\theta(x) = 0$ for otherwise, $\mathbf{x}_i$ and ω_i are respectively the position and the angular velocity of $i-$th particles. $\mathbf{n}$ and $\mathbf{t}$ are respectively the unit normal and unit tangential vector in the contacted pair of particles. The forces $\tilde{\mathbf{F}}_n^{ij}$ and $\tilde{\mathbf{F}}_t^{ij}$ are given by

$$\begin{aligned} \tilde{\mathbf{F}}_n^{ij} &= \mathbf{F}_n^{ij} - \eta_n \mathbf{n}\mathbf{n} \cdot (\dot{\mathbf{x}}_i - \dot{\mathbf{x}}_j) \\ \tilde{\mathbf{F}}_t^{ij} &= \begin{cases} \mathbf{F}_{t,nsl}^{ij} & (\text{for } |\mathbf{F}_{t,nsl}{}^{ij}| < \mu\tilde{\mathbf{F}}_n^{ij}) \\ \mu\tilde{\mathbf{F}}_n^{ij} & (\text{otherwise}) \end{cases} \\ \mathbf{F}_{t,nsl}^{ij} &= \mathbf{F}_t^{ij} - \eta_t \mathbf{t}[\mathbf{t} \cdot (\dot{\mathbf{x}}_i - \dot{\mathbf{x}}_j) + \frac{d}{2}(\omega_i + \omega_j)], \end{aligned} \tag{2·4}$$

where $\mathbf{F}_n^{ij}, \mathbf{F}_t^{ij}$ are $\mathbf{F}_n, \mathbf{F}_t$ in eqs. (2·1),(2·2) for i-j pairs.

Following Cundall and Strack[7] we assume the critical damping condition as $\eta_n = 2\sqrt{mk_n(\delta_n)}$ and $\eta_t = 2\sqrt{2mk_t(\delta_n)/5}$. We further assume $d = 1$ cm, $\rho = 2.5$ g/cm^3, $E = 5 \times 10^9$ Pa, $\mu = 0.45$, $\sigma_0 = 0.25$. We introduce a spatially fixed particles at the bottom. There is a top plate consisting of particles where all particles are connected by a rigid string. The top plate is connected with a motor which pushes the plate $V = 0.45\sqrt{gd}$ by a Hookian spring (its spring constant is $k = 20mg/d$). The plate is compressed by the pressure $P = 40mg/d$ per unit length. We adopt the

second order Euler scheme with a constant $dt = 10^{-4}\sqrt{d/g}$. All of parameters are similar to those of actual situations and those by Thompson and Grest[8]. Numer of particles in our simulation is between 500 and 1000.

Here we only present preliminary results. Details will be reported elsewhere. From fig.1 we can see that we reproduce stick-slip motion from our simulation. Although we do not present explicit figures here, we can draw the stress network from the force acting at each contact point where the contacted pairs can be specified. From the observation of stress network, it is easy to characterize the slip transition as a broken process of stress network.

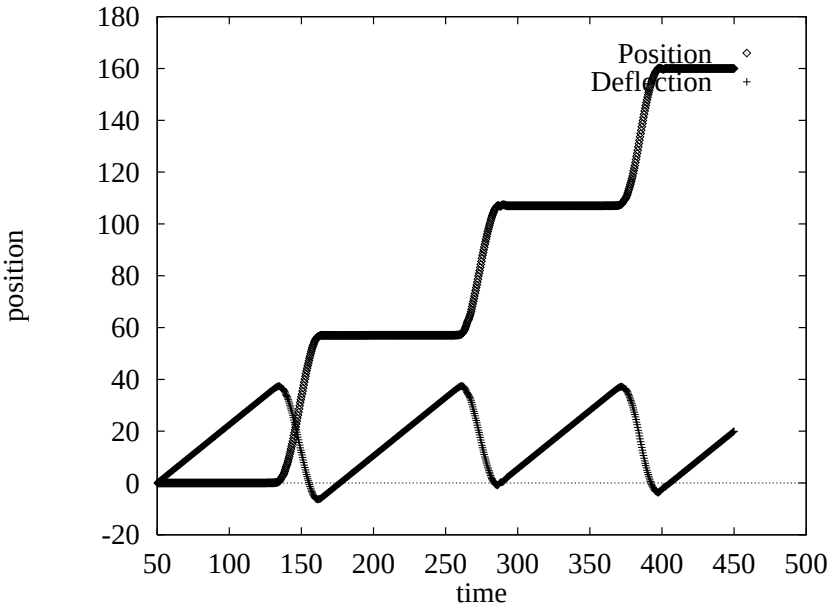

Fig. 1. An example of stick-slip motion obtained from DEM simulation. Time and position are dimensionless quantities with dividing by $\sqrt{d/g}$ and d, respectively. Position and Deflection represent the horizontal position of the center of mass of the plate, and the deflection of the spring, respectively.

Unfortunately, we must confess ourselves that we cannot obtain stable stick slip motions in wide parameter regions. Even in the result in Fig.1 the deflection becomes negative which has not been observed in any experiment[3]. For example, if we replace the bottom fixed particles by a flat elastic plate, we cannot obtain any stick-slip motion. The situations are similar if (i) we replace the top plate by a flat plate, and (ii) we introduce the randomness in size distribution of particles. The instability of stick-slip motion may come from the introduction of the rotation of particles which are omitted in former simulations[8),9)]. It may be important to consider the rotational friction[12]. Thus, we may have room for improvement of the DEM model.

§3. Phenomenological Model

Hayakawa[6] proposed a phenomenological model to explain the experiment by Nasuno et al[3] as an extension of that by Carlson and Batista[13]. Here we briefly explain his model and result of his simulation.

Let the mass of the plate be M. We assume that the friction between granular layers and the plate is characterized by the order parameter θ, where $\theta = 1$ represents solid-like state. (Namely, θ can be considered as the fraction of connecting stress network from the top plate to the bottom particles). The plate is pushed by a driving motor with the constant speed V, which is connected with the motor by a Hookian spring (the spring constant k).

Thus, the equations of the plate is given by

$$M\ddot{x} = k(Vt - x) - \frac{\partial}{\partial x}W - \mu MgFr\left(\frac{\dot{x}}{u_0(V)}\right), \tag{3·1}$$

where g and μ are respectively the gravitational acceleration and the dynamical friction constant. We adopt the friction force $Fr(x)$ as

$$Fr(x) = \tanh(x) \quad \text{for } x > 0, \quad Fr(x) = b_0 x \quad \text{for } x < 0, \tag{3·2}$$

where we assume that b_0 is a large constant, which essentially inhibits the motion with negative velocity. Note that the saturation of the friction in $\tanh(x)$ for large velocity corresponds to the Coulomb's friction law as in DEM model[7),8)]. The potential W is given by

$$W = \frac{k\theta\xi^2}{2}\left[1 - \exp\left(-\frac{(Vt - x)^2}{\xi^2}\right)\right], \tag{3·3}$$

which is a resistance force in solid-like state. We adopt here the Gaussian-Taguchi model introduced in simulation of fracture mechanics[14]. The reason why we introduce a continuous fracture model is (i) to represent precursor events before main slips and (ii) to represent a state in which stress networks are partially broken. Note that in our model the static friction is not introduced explicitly but is replaced by the fracture mechanism of stress network.

It is obvious, as in eq.(3·3), that the stress network plays no roles in a liquid-like state but plays an essential role in a solid-like state. Thus we introduce the equation of the order parameter as

$$\tau\dot{\theta} = \Theta(\theta, a(\dot{x})) - \frac{\partial W}{\partial \theta} - \zeta(V)\theta\dot{x}, \tag{3·4}$$

where τ is a characteristic time scale. The first term $\Theta(\theta, a) \equiv \theta(\theta - a(\dot{x}))(1 - \theta)$ in the right hand side of (3·4) represents the dynamics of 'liquid-solid transition', where θ increases (decreases) when $\Theta > 0$ ($\Theta < 0$). The point at which satisfies $\Theta = 0$ is a fixed point. A double root point of $\Theta = 0$, or Θ is an increasing function of θ at a fixed point, the fixed points are unstable, while other cases at $\Theta = 0$ are stable fixed points. In eq.(3·4), $a(\dot{x})$ is assumed to be a function of sliding velocity, where we

adopt $a(\dot{x}) = \tanh^2(\dot{x}/v_0)$ with a characteristic velocity v_0 to satisfy the following properties. When there is no sliding, the system should be in a solid state. While the system should be in a liquid state when the sliding velocity is infinite. For finite velocity, both two (liquid and solid) states become locally stable, and $\theta = a(\dot{x})$ is an unstable fixed point. The model (3·4) describes such the process. We also assume $\zeta(V) = \zeta_0/\tanh(V)$ and $u_0(V) = \bar{u}\tanh(V)$ in dimensionless unit with $\bar{u} = \zeta_0 = 0.1$. The last term in (3·4) represents shear-induced melting force[13].

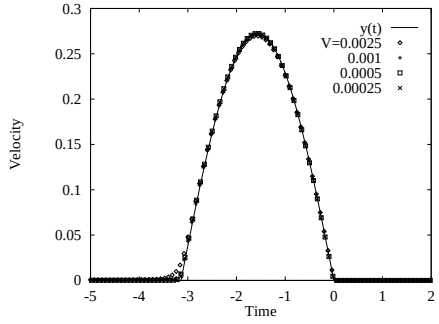

Fig. 2. Instantaneous dimensionless velocity $\frac{d\hat{x}}{d\hat{t}}$ as a function of dimensionless time $\hat{t}$ during slip in the stick-slip regime. The origins of the pulses are forced to agree at the end of each event. The solid curve is $-0.272\sin(\hat{t})$ which is obtained by the classical Amontons-Coulomb's law.

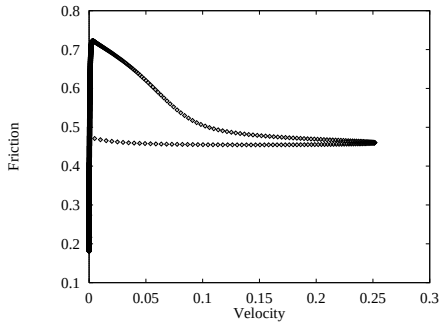

Fig. 3. The hysteresis loop of the friction force $\frac{d^2\hat{x}}{d\hat{t}^2} - (\hat{V}\hat{t} - \hat{x})$ in dimensionless unit as a function of dimensionless slip velocity $d\hat{x}/d\hat{t}$ for driving speed $\hat{V} = 0.01$.

All of simulations are carried out in dimensionless unit, where the variables in the unit of space, time, and velocity are respectively scaled by Mg/k, $\sqrt{M/k}$, and $g\sqrt{M/k}$. Here, we restrict our interest to the case for $k = 135$ N m^{-1}, $M = 1.1\times10^{-2}$ kg, $g = 9.8$ m/s^2, and $\mu = 0.45$. For later discussion the variables with hat are dimensionless ones. In Fig.2, we plot the profile of slip velocity, where $\hat{t} = 0$ is fixed at the end of slip events. All the data between $\hat{V} = 2.5\times10^{-4}$ and 2.5×10^{-3} seem to be on a universal curve as in the experiment. Although we can observe stick-slip motion for larger V, the profile depends on $\hat{V}$ in such regions. Even in universal region, we can find a non-universal part of the profile near the start of slip, where the velocity has the larger for large $\hat{V}$ value than that for small $\hat{V}$. In Fig.3, we plot the dimensionless frictional force $\frac{d^2}{d\hat{t}^2}\hat{x} - \hat{V}\hat{t} - \hat{x}$ as a function of slip velocity. As in Fig.3 we obtain a hysteresis loop for the friction which is similar to that observed in the experiment. Hysteresis loops, however, depend on $\hat{V}$ in our model, where the area of the hysteresis becomes narrower when the driving velocity becomes slower.

Hayakawa[6] reported that the area of hysteresis loop obeys

$$S \simeq c\hat{V}^{\alpha}, \quad c = 0.248, \quad \alpha = 0.547 \pm 0.033. \tag{3·5}$$

However, nobody has reported this law from experiments and simulations. We need further investigation on this problem.

§4. Concluding Remarks

In this paper we examine the application of the distinct element method (DEM) for granular friction and its effective (or simplified) macroscopic models. We focus on the stick-slip motion in a sheared granular friction process and reproduce many of the experimental results [3] from the simulations of the DEM model and the effective model.

There are some unclear points in our preliminary work. (i) Why is stick-slip motion so unstable? This process may be a serious and good test for the validity of DEM. Thus, we will have to refine the DEM model. (ii) In the phenomenology, how to define the order parameter θ in quantitative sense. We may need to rewrite it as a field variable. (iii) Is it true that the area of hysteresis loop depends on the driving velocity V? We may have creep motions in very slow V region in actual systems, while we suppress such the process in our phenomenology. (iv) What is the breaking mechanism of slip motion? In our phenomenology we include such the mechanism by hand, while it is not easy to understand its mechanism from DEM. These points should be clarified in near future.

Acknowledgments

The author would like to thank A. Shimosaka, T. Umekage and S. Yuu for helpful discussion on the simulation code of DEM model. I also appreciate comments by K. Ichiki and M. Isobe. This work is partially supported by Grant-in-Aid for Science Research Fund from the Ministry of Education, Science and Culture (No. 11740228).

References

1) H. M. Jaeger, S. R. Nagel and R. P. Behringer,Rev. Mod. Phys. **68** (1996), 1259.
2) B. N. J. Perrson, Sliding Friction : Physical Principle and Applications (Springer, Berlin, 1998)
3) S. Nasuno, A. Kudrolli, A. Bak and J. P. Gollub,Phys. Rev. **E58** (1998), 2161
4) F. Heslot, T. Baumberger, B. Perrin, B. Caroli and C. Caroli,Phys. Rev. **E49** (1994), 4973
5) K. Sato and A. Toda, J. Phys. Soc. Jpn. **68** (1999), 75
6) H. Hayakawa, Phys. Rev. **E60** (1999), 4500
7) P. A. Cundall and O. D. L. Strack, Geotechnique, **29** (1979), 47
8) P. A. Thompson and G. S. Grest, Phys. Rev. Lett. **67** (1991), 1751
9) T. Matthey and J. P. Hansen, Mod. Simul. Mater. Sci. Eng. **6** (1998) 701
10) A. E. Love, A Treatise on the Mathematical Theory of Elasticity (Dover, New York, 1926)
11) R. D. Minlin, J. Appl.Mech. Trans. ASME **16**, (1949) 259: R. D. Minlin & H. Deresiewicz, J. Appl.Mech. Trans. ASME **20** (1953), 327 .
12) Y. C. Zhou, B. D. Wright, R. N. Yang, B. H. Xu and A. B. Yu, Physica A **269** (1999) 536
13) J. M. Carlson and A. A. Batista, Phys. Rev. E **53**, 4153 (1996); A. A. Batista and J. M. Carlson, Phys. Rev. E **57**, 4986 (1998).
14) Y-h. Taguchi, Mod. Phys. Lett. B **8**, 1335 (1994).